FEASIBILITY STUDY FOR A SEEDED HARD X-RAY SOURCE BASED ON A TWO-STAGE ECHO-ENABLED HARMONIC GENERATION FEL*

D. Xiang†, Z. Huang, D. Ratner and G. Stupakov, SLAC, Menlo Park, CA 94025 USA

Abstract

We propose and analyze a scheme to achieve a seeded hard x-ray source based on a two-stage echo-enabled harmonic generation (EEHG) FEL. In the scheme an 180 nm seed laser covering the whole bunch is first used to modulate the beam when beam energy is 2 GeV. After passing through a strong chicane complicated fine structures are introduced into the phase space. The beam is again modulated by a short 180 nm laser that only interacts with the rear part of the beam and accelerated to 6 GeV. A chicane is then used to convert the energy modulation imparted to the rear part of the beam into density modulation. The density-modulated beam is sent through a radiator to generate intense 6 nm radiation which will be used to interact with the front fresh part of the bunch. Finally we generate in the front part of the beam density modulation at the 1199th harmonic of the seed laser. We will discuss the issues related to the realization of the seeded hard x-ray FEL.

INTRODUCTION

LCLS, the world's first SASE-based hard x-ray FEL at SLAC, has achieved saturation at 1.5 Å [1] and will provide unprecedented powerful x-rays for the users this year. Because SASE starts from electron beam shot noise, such a source has limited temporal coherence and relatively large shot-to-shot statistic fluctuations. There are many applications (e.g. studies of slow vibrational modes in biological membrane, ultrahigh resolution spectroscopy, etc) that require or could benefit from an improved temporal coherence in the x-ray pulses.

In this paper we study the feasibility of generating hard x-ray pulse with good temporal coherence using a two-stage EEHG FEL [2-3]. In the EEHG FEL, the beam is first energy modulated in a modulator and then sent through a dispersion section with strong dispersion strength after which the modulation obtained in the first modulator is washed out while simultaneously complicated fine structures (separated energy bands) are introduced into the phase space. A second laser is used to further modulate the beam energy in the second modulator. After passing through the second dispersion section the separated energy bands will convert to separated current bands which contain considerable higher harmonic of the seed laser.

The EEHG scheme has a remarkable up-frequency conversion efficiency and allows generation of coherent soft x-rays in the water window directly from a UV seed laser in a single stage [4]. In this paper we study the feasibility of extending the radiation wavelength to hard x-ray range using a two-stage EEHG FEL integrated in a novel way. We will discuss the issues related to the realization of the seeded hard x-ray source using the proposed two-stage EEHG FEL.

METHODS

The schematic of the two-stage EEHG FEL is shown in Fig. 1. In the scheme an 180 nm seed laser covering the whole bunch is first used to modulate the beam in M1 when beam energy is $E_1 = 2$ GeV. After passing through a strong dispersion section (D1) the beam is again modulated by a short 180 nm laser that only interacts with the rear part of the beam in M2. The beam is then accelerated to $E_2 = 6$ GeV in the linac. After passing through a weak dispersion section (D2), the rear part of the beam will be bunched at the 30th harmonic of the seed laser (6 nm). Intense 6 nm radiation will be generated in a radiator (R1) from the rear part of the beam. The beam is then time-delayed and the 6 nm radiation is further used to modulate the fresh front part of the beam in M3. After passing through another weak chicane (D4), the beam is bunched at the 1199th harmonic of the seed laser and finally coherent hard x-ray radiation at 1.5 Å is achieved in the long radiator R2.

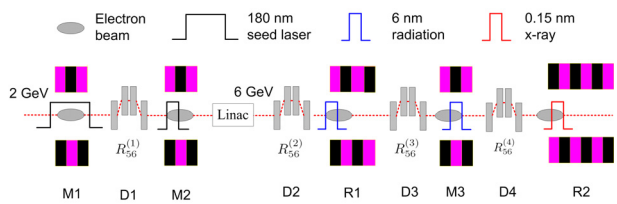

Figure 1: Schematic of the proposed seeded hard x-ray source based on a two-stage EEHG FEL.

The reason why we choose to modulate the beam with the UV seed laser at 2 GeV is two fold. First, 2 GeV beam is suitable for soft x-ray FEL. We'd like to reserve the flexibility of extracting the beam after M2 and use it to drive a seeded soft x-ray FEL. The other reason is to mitigate the quantum diffusion effect in both the dipoles and undulators (see next section for detail). The main parameters for the seeded hard x-ray FEL are listed in Table. 1.

Following the notation of [2,3], we assume an initial Gaussian beam energy distribution with an average energy E_0 and the rms energy spread σ_E, and use the variable $p = (E - E_0)/\sigma_E$ for the dimensionless energy deviation of a particle. In our scheme, E_0 varies after the linac. The initial longitudinal phase space distribution can then be written as $f_0(p) = N_0(2\pi)^{-1/2}e^{-p^2/2}$, where N_0 is

* Work supported by US DOE contracts DE-AC02-76SF00515.
† dxiang@slac.stanford.edu

Table 1: Main parameters for the seeded hard x-ray FEL

Beam energy at M1 and M2	2 GeV
Beam energy at R1, M3 and R2	6 GeV
Peak current	2 kA
Duration of the flat part of the beam	400 fs
Normalized emittance	1 mm mrad
Slice energy spread	300 keV
$R_{56}^{(1)}$	1.50 mm
$R_{56}^{(2)}$	144 μm
$R_{56}^{(3)}$	120 μm
$R_{56}^{(4)}$	4.24 μm
$N_p \times \lambda_u$ for M1	4 $\times$20 cm
$N_p \times \lambda_u$ for M2	5 $\times$20 cm
$N_p \times \lambda_u$ for R1	100 $\times$20 cm
$N_p \times \lambda_u$ for M3	29 $\times$20 cm
Seed laser peak power for M1	5 GW
Energy modulation in M1	0.90 MeV
Energy modulation in M2	1.20 MeV
Energy modulation in M3	1.45 MeV
Radiation power at the exit of R1	1.2 GW

the number of electrons per unit length of the beam. After some mathematical manipulations, the longitudinal phase space for the rear part of the beam at the exit of the second dispersion section is,

$$f_r(\zeta,p) = \frac{N_0}{\sqrt{2\pi}}\exp\Big[-\frac{1}{2}\big(p - A_2^r\sin(\zeta - B_2^r p) - A_1^r\sin(\zeta-(B_1^r+B_2^r)p + A_2^rB_1^r\sin(\zeta - B_2^r p)\big)\big)^2\Big]. \quad (1)$$

where $\zeta = k_1 z$, k_1 is the wave number of the UV seed laser in M1 and M2, $B_1^r = k_1 R_{56}^1 \sigma_E/E_1$, $B_2^r = k_1(R_{56}^{(L)}\sigma_E/E_1 + R_{56}^{(2)}\sigma_E/E_2)$, $R_{56}^{(1)}$, $R_{56}^{(2)}$ and $R_{56}^{(L)}$ are the dispersion strength for D1, D2 and the linac, E_1 and E_2 are the beam energy at the first dispersion and second dispersion section, respectively. The optimized bunching factor for the rear part beam is,

$$b_h = |J_{h+1}\left(hA_2^rB_2^r\right)J_1\left(A_1^r(hB_2^r - B_1^r)\right)| \exp\left[-\frac{1}{2}(hB_2^r - B_1^r)^2\right], \quad (2)$$

To generate the 30th harmonic of the seed laser in R1, we choose $A_1^r = 3$, $A_2^r = 4$, $B_1^r = 7.85$ and $B_2^r = 0.28$. The longitudinal phase space evolution for the bunch in M1, M2, D1 and D2 are simulated with our 1-D code and the results are shown in Fig. 2. Fig. 2c shows the phase space of the beam at the exit of M2 where one can see that the rear part of the beam is energy modulated with $A_2^r = 4$ while the phase space for the front part of the beam is almost unchanged. A linac is further used to boost the beam energy to 6 GeV. Note p is defined as the dimensionless energy deviation of a particle with respect to the reference particle, therefore p does not change after the linac. The 6 GeV beam is then sent through D2 after which the rear part of the beam is effectively bunched while only separated energy bands are present for the front part of the beam, as illustrated in Fig. 2d. The rear part of the beam will generate intense radiation at 6 nm when sending it through R1 tuned to the 30th harmonic of the UV seed laser.

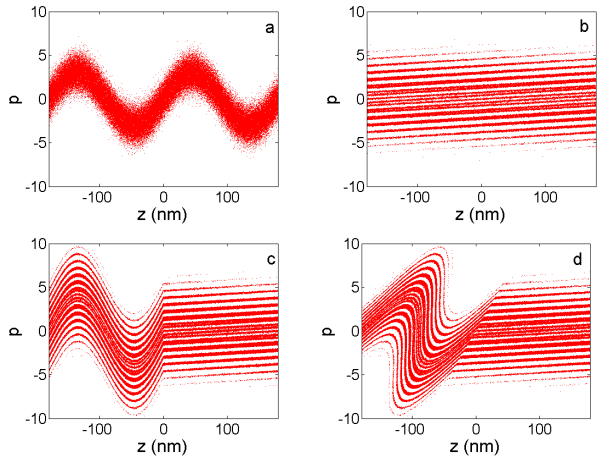

Figure 2: Longitudinal phase space evolution (z<(>)0 for the rear (front) part of the beam): (*a*) at the exit of M1; (*b*) at the exit of D1; (*c*) at the exit of M2; (*d*) at the exit of D2.

The phase space for the electrons in the front part of the beam at the entrance to the final radiator can be similarly found,

$$f_f(\zeta,p) = \frac{N_0}{\sqrt{2\pi}}\exp\Big[-\frac{1}{2}\big(p - A_2^f\sin(\kappa\zeta - \kappa B_2^f p) - A_1^f\sin(\zeta-(B_1^f+B_2^f)p + A_2^fB_1^f\sin(\kappa\zeta - \kappa B_2^f p)\big)\big)^2\Big]. \quad (3)$$

where $\kappa = k_2/k_1$, k_2 is the wave number of the radiation in M3, $B_2^f = k_1 R_{56}^{(4)}\sigma_E/E_2$, and

$$B_1^f = k_1\big[(R_{56}^{(2)} + R_{56}^{(3)} + R_{56}^{(R_1)})\frac{\sigma_E}{E_2} + (R_{56}^{(1)} + R_{56}^{(M_2)} + R_{56}^{(L)})\frac{\sigma_E}{E_1}\big]. \quad (4)$$

where $R_{56}^{(L)} = L/\gamma_1\gamma_2$ is the dispersion strength of the linac, L is the length of the linac, γ_1 and γ_2 are the beam energy at the entrance and exit of the linac; $R_{56}^{(M_2)}$ and $R_{56}^{(R_1)}$ are the dispersion strength in M_2 and R_1, respectively. The optimized bunching factor for the harmonic number $h = n + \kappa m$ is,

$$b_{n,m} = |J_m\left((\kappa m+n)A_2^fB_2^f\right) \times J_n\left(A_1^f(nB_1^f + (\kappa m+n)B_2^f)\right)| \times \exp\left[-\frac{1}{2}(nB_1^f + (\kappa m+n)B_2^f)^2\right], \quad (5)$$

The front part of the beam is energy modulated with the 6 nm radiation generated in R1, so we have $\kappa = 180/6 = 30$. Take $n = -1$, $m = 40$, one can maximize the bunching factor for the 1199th harmonic using Eq. (5). The dispersion strength of an undulator is $2N_p\lambda_r$, where λ_r is the resonant wavelength of the undulator. The dispersion strength for the delay chicane is about $2ct_d$, where t_d is the delay time introduced by the chicane. In our example the delay time is about 200 fs which corresponds to half the length of the flat part of the beam. For the front part of the electrons, we have $A_1^f = 3$ and $B_1^f = 8.35$. Using Eq. (5) we found that the bunching factor for the 1199th harmonic is maximized when $A_2^f = 4.82$ and $B_2^f = 0.00741$. The longitudinal phase space for the front part of the electrons and the corresponding bunching factor at various harmonic numbers are shown in Fig. 3 where one can see the bunching factor is about 0.1 for the 1199th harmonic. It can be anticipated that powerful coherent radiation at 1.5 $\mathring{A}$ will be generated when sending the beam to R2.

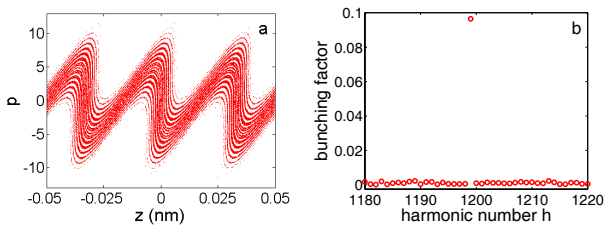

Figure 3: Phase space at the entrance to R2 (a) and the corresponding bunching factor (b).

PRESERVATION OF THE FINE STRUCTURES

To make the proposed seeded hard x-ray FEL work, the fine structures must be preserved from the exit of M1, through M2, the linac, D1, D2, etc and up to the final radiator. The finite size of the laser and the quantum fluctuations in the process of ISR lead to diffusion in energy. Analysis shows that the spacing of the adjacent energy bands is on the order of $(\pi/B_1)\sigma_E$, corresponding to about 120 keV in our example. If the rms value of the energy spread caused by these diffusions exceeds the spacing of two adjacent energy bands, it may result in the overlapping of the bands, which will wash out the fine structures of the longitudinal phase space and thus degrade the FEL performances. The second order transportation effect from the transverse emittance also tends to wash out the fine structures which deserves special attention considering the long transportation distance in the linac.

Finite laser and radiation size

Due to the finite size of the laser beam, electrons with different radial positions will see the laser field of various amplitudes, which will cause a local energy spread growth which is found to be,

$$\Delta\sigma_E = \frac{\sqrt{2}A\sigma_E}{2}\left[\frac{1}{1+\sigma_x^2/\sigma_r^2} - \frac{1}{(1+\sigma_x^2/2\sigma_r^2)^2}\right]^{1/2}, \quad (6)$$

where we assumed a round beam and σ_x and σ_r are the horizontal rms size of the electron beam and laser beam, respectively. In order to make the condition $\Delta\sigma_E < (\pi/B_1)\sigma_E$ satisfied, one typically requires the laser size to be much larger than the electron beam size. The condition can be easily satisfied for the UV seed laser. But for the 6 nm radiation whose size is comparable to the electron beam size in R1, one may need to use a relatively large electron beam size in R1 and reduce the electron beam size in M3 to make the condition satisfied. In our example the beam size in R1 is about 90 μm and the distance between R1 and M3 are comparable to the Rayleigh length so that in M3 the radiation size is about 180 um, much larger than the electron beam size in M3 which is about 40 μm.

Quantum diffusion

The quantum diffusion effect in D1, D2 and D3 are most serious: D1 has the largest R_{56} among all the dispersive elements; as for D2 and D3, even though their R_{56} are much smaller than that of D1, the beam energy is much higher. In D1 the required dispersion strength is $B_1^r = 7.85$ corresponding to $R_{56}^{(1)} = 1.50$ mm. As an example, we consider a 4-dipole symmetric chicane. The length of the dipole L_b and the distance between dipoles L_d are assumed to be 0.4 m and 0.5 m, respectively. The energy spread growth caused by ISR for D1 is found to be about $\Delta\sigma_E = 1.4$ keV. For the delay chicane, assuming a 200 fs delay time, its strength is about $R_{56}^{(3)} = 0.12$ mm. Assuming $L_b = L_d = 1$ m for both D2 and D3, the local energy spread growth is found to be about 2.6 keV and 2.2 keV for D2 and D3, respectively.

The quantum diffusion in the undulators is also able to wash out the separated energy bands [5]. Analysis shows that the quantum diffusion strongly depends on beam energy and undulator strength. Assuming an undulator period length of 20 cm, the local energy spread growth in M2 is about 0.73 keV. The quantum diffusion in R1 and M3 are, however, much more serious, because of the high beam energy. The longer radiator gives higher power which requires a shorter modulator to achieve the required energy modulation. Similarly a short radiator gives lower power and thus needs a long modulator to achieve the same energy modulation level. The criterion to determine the radiator and modulator lengths is to find a set of parameters that give a small energy spread growth from quantum diffusion while also limiting the undulator length to a reasonable value. After some optimization, the length of R1 and M3 are chosen to be 20 m and 5.8 m, and the corresponding local energy spread in R1 and M3 are found to be 13.6 keV and 4.2 keV, respectively. The total local energy spread growth is found to be $\Delta\sigma_{E,tot} \approx 14.7$ keV.

High order transportation effects

In addition to the energy diffusion, the second order transportation effects from transverse emittance also tends to wash out the fine structures [6]. If the longitudinal position change caused by second order effect exceeds the spacing of the fine structures, it will cause significant degradation. The spacing of the fine structures for the rear part of the beam is comparable to the harmonic radiation wavelength (6 nm) and that for the front part of the beam is comparable to the laser wavelength (180 nm), therefore the fine structures in the rear part of the beam is more vulnerable.

ELEGANT [7] is used to address the high order transportation effects in the linac which boosts the beam energy from 2 GeV to 6 GeV. We used the standard SLAC 3-meter S-band acceleration structure and assume an acceleration gradient of 18 MV/m. A FODO lattice is used to focus the beam in the linac with an average Beta function of 100 m. The total transportation length from M2 to D2 is assumed to be 250 m.

To mitigate the smearing from finite laser size, the beam has an average Beta function of 20 m in M1 and M2. A matching section is used to match the beam to the linac where the average Beta function is 100 m. Efforts have been devoted to make a smooth transition of the Beta function in the matching section to reduce the second order aberration. The beam is tracked with ELEGANT from M1 to D2 and the phase space of the beam at the exit of D2 is shown in Fig. 4.

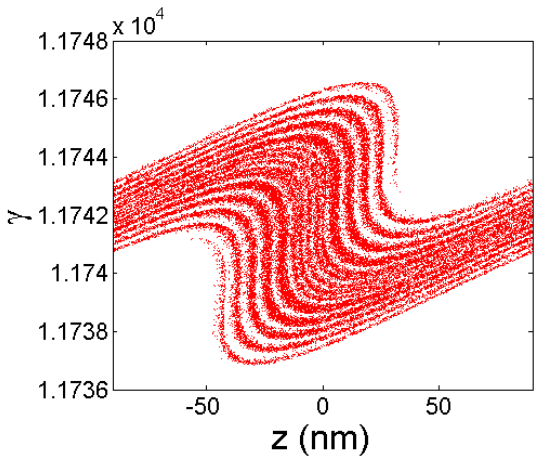

Figure 4: Longitudinal phase space of the beam at the exit of D2.

It is found that the emittance does have some smearing effect on the fine structures, but with proper design of the lattice, one can still get sufficient bunching at the 30th harmonic of the seed laser after D2. Detailed tracking studies indicate that the smearing is mainly due to the particles that have large Betatron amplitude which tends to lag behind the reference particle. In principle it can be compensated by beam conditioning technique [8] which gives the particle that has large Betatron amplitude more energy to compensate the average velocity difference.

S/N RATIO DEGRADATION

While the theory of noise amplification in the EEGH FEL is not available at this time, we can try to estimate the signal to noise (S/N) ratio in this case using HGHG formula from Ref. [10],

$$P_{sn} \approx \frac{\lambda_u N_u r_e \sigma_L^2}{8\sigma_x^4} \frac{K^2[JJ]^2}{1+K^2/2} \frac{mc^2}{e} I\,, \qquad (7)$$

where λ_u is the undulator period in the modulators and σ_L is the rms laser size. Eq. (7) indicates that it is desirable to modulate the beam at moderate energy to reduce the effective shot noise power and simultaneously increasing the laser power and laser size does not increase the S/N ratio. For a 2 GeV beam with 2 kA peak current and average Beta function of 20 m, the effective shot noise power at 180 nm in the modulator is about 1 kW. The S/N ratio will be reduced by at least 1199^2 [9,10], so a seed laser with peak power of a few GW is needed in order to generate coherent hard x-ray pulse with S/N ratio much larger than unity. In our example rough estimation gives a S/N of about 4 for the 1.5 Å radiation. It is worth pointing out that the signal radiation has a much narrower bandwidth than the noise radiation. Therefore one can in principle use a monochromator to filter out most of the noise radiation and significantly increase the S/N ratio.

More systematic work is being conducted to study the FEL performances and analyze the S/N degradation for the EEHG FEL and will be reported elsewhere.

ACKNOWLEDGEMENTS

We thank M. Borland, A. Chao, H. Geng and Y. Nosochkov for helpful discussions.

REFERENCES

[1] P. Emma, PAC'09, TH3PBI01 (2009); P. Emma, FEL'09, These proceedings.

[2] G. Stupakov, Phys. Rev. Lett, 102 (2009) 074801.

[3] D. Xiang and G. Stupakov, Phys. Rev. ST-AB, 12 (2009) 030702.

[4] D. Xiang and G. Stupakov, PAC'09, to be published; see also SLAC-PUB-13645 (2009).

[5] D. Xiang and G. Stupakov, PAC'09, to be published; see also SLAC-PUB-13644 (2009).

[6] D. Ratner, A. Chao and Z. Huang, FEL'09, These proceedings.

[7] M. Borland, "Elegant: A flexible SDDS-compliant code for accelerator simulation," Advanced Photon Source LS-287, September, (2000).

[8] A. Sessler, D. Whittum and L.H. Yu, Phys. Rev. Lett, 68 (1992) 309.

[9] E. Saldin, E. Schneidmiller, and M. Yurkov, Opt. Commun. 202 (2002) 169.

[10] Z. Huang, FEL'06, p. 130 (2006).